Effect of particle size on flotation performance of hematite

Ximei Luo [1,2], Shuixiang Song [1,2], Mingze Ma [1,2], Yunfan Wang [3], Yongfeng Zhou [1,2], Ying Zhang [1,2]

[1] State Key Laboratory of Complex Nonferrous Metal Resources Clean Utilization, Kunming University of Science and Technology, Kunming 650093, China

[2] Faculty of Land and Resource Engineering, Kunming University of Science and Technology, Kunming 650093, China

[3] Faculty of Minerals Processing and Bioengineering, Central South University, Changsha 410083, China

Corresponding authors: 85128225@163.com (X.M. Luo), asc_cloud@aliyun.com (Y.F. Wang)

Abstract: The effect of particle size on flotation performance of hematite and quartz was investigated. Microflotation, X-ray photoelectron spectroscopy analysis, reagent adsorption measurements, and collision and attachment probability calculation between particle and bubble were conducted in this investigation. The results showed that the floatability of minerals with different particle size fractions was different, which was mainly related to surface bonding site, reagent adsorption, collision probability and entrainment. The quartz with different particle size had little impact on hematite recovery, but -45 μm fraction negatively affected Fe grade of concentrate both in the direct and reverse flotation of hematite. In the direct flotation, the Fe grade in froth product dropped off due to the fine quartz entrainment. While in the reverse flotation, the Fe grade in sink product dropped off as a result of difficulty in floating fine quartz particles, which was due to lower collision probability. Meanwhile, in the reverse flotation, the presence of hematite fines (-18 μm fraction) also had negative impact on hematite recovery because of fine particle entrainment.

Keywords: particle size, hematite, entrainment, surface bonding site, reagent adsorption

1. Introduction

Froth flotation technology is an important concentration process in the separation of quartz from hematite during iron ore beneficiation (Ma et al., 2011; Liu et al., 2018). Three main routes for iron ore beneficiation through flotation, namely reverse cationic flotation, direct anionic flotation and reverse anionic flotation were described by Araújo et al. (2005). In China, anionic flotation is often employed according to iron ore characteristic and technological conditions (Chen and Zhang, 2013). For direct flotation, hematite can be floated with fatty acid as collector, while silicate minerals are depressed. For the reverse flotation, hematite is depressed with the help of starch, and the silicate minerals (such as quartz) are floated by using calcium ion as activator of quartz and fatty acid as collector under strong alkaline conditions (Kar et al., 2013; Shrimali et al., 2018; Shrimali et al.,2016b).

Ores must be ground to very fine particles to facilitate sufficient liberation of valuable minerals. However, the grade and recovery of valuable minerals in concentrate declines sharply when operating in the fine particle size ranges (<45 μm) (Han et al., 2015; Li et al., 2016; Shrimali et al.,2016a). A large number of studies has been carried out to improve the recovery of fine hematite, such as carrier flotation (Qiu et al., 1994), flocculation flotation (Ng et al., 2015; Yang, et al., 2013; Yin et al., 2011; Forbes, 2011; Shibata and Fuerstenau, 2003) and dispersion flotation (Luo et al., 2016; Yin et al., 2013).

In recent years, researchers have increasingly paid more attention to the effect of particle size on the flotation process. Pérez-Garibay et al. (2014) studied the effect on sphalerite flotation of the feed and bubble size distributions, superficial air velocity and collector dosage. Results showed that the recovery highly depended on these factors. The carrying capacity of the smaller bubbles was higher for the fine

than for the coarser sphalerite. Vieira et al. (2007) studied the flotation performance of quartz particles of different size range in the presence of ether monoamine and ether diamine. The results indicated that ether diamine performed better in the flotation of medium and coarse quartz, while ether monoamine was more effective in the case of fine quartz, and also that the flotation performance of coarse particles was enhanced in the presence of fine particle in the system. Pita et al. (2017) indicated that floatability differed with the size and shape of plastic particles; for regular-shaped plastics floatability decreased with the increase of particle size, while for lamellar-shaped particles floatability was slightly greater for coarser particles; thus, plastic particles with small size, lamellar shape and low density presented a greater floatability. The effects of gangue mineral particle size on the recovery of fine (10-50 µm) and ultrafine (<10 µm) valuable mineral particles was investigated by Leistner et al. (2017). The results showed that the flotation performance of ultrafine magnetite was similar to fine magnetite when the gangue particles were fine as well. On the contrary, the recovery of fine magnetite dropped sharply when ultrafine quartz was used as the gangue mineral system. Norori-McCormac et al. (2017) studied the effect of particle size distribution on froth stability in flotation. Yin and Wang (2014) explored the effect of size distribution on scheelite flotation. They found that particle size affected the scheelite recovery and the performance of combined reagents. The scheelite recovery decreased after adding fine particles (<10 µm) into the pulp containing coarse particles.

Even though the flotation of fine hematite has been formerly investigated, the flotation performance data for a number of hematite particle size fractions is limited. In this study, the influence of particle size on flotation performance of single mineral and mixed minerals were investigated. Microflotation, X-ray photoelectron spectroscopy analysis, reagent adsorption measurements, and collision and attachment probability between particle and bubble calculation were conducted in the investigation. These findings are expected to be helpful to the research of hematite flotation.

2.   Materials and methods

2.1. Materials

The hematite sample was obtained from Anshan City, Liaoning Province, China. The quartz sample was purchased from Yingkou City, Liaoning Province, China. The hematite and the quartz samples were carefully hand-picked, crushed, ground, processed by gravity concentration and wet sieved to obtain size fractions in the range of −106+45 µm, -45+18 µm and −18 µm, which were employed for microflotation experiment, reagent adsorption and X-ray photoelectron spectroscopy measurements. X-ray diffraction (Fig. 1 and Fig. 2) and chemical element analyses (Table 1) showed that hematite and quartz samples were of high purity. The hematite and quartz samples contained about 67.45% Fe and 99.77% SiO_2, respectively.
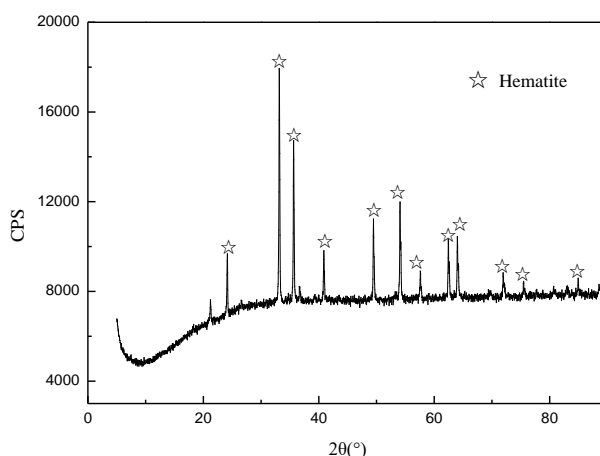
Fig. 1. X-ray diffraction spectrum of hematite

2.2. Reagents

Sodium oleate, calcium chloride and corn starch with more than 98% purity were used as anionic collector, quartz activator and the depressant of iron minerals, respectively. Corn starch was dissolved

in distilled water by adding 20 wt.% NaOH at 50 °C on a hot plate. Analytical grade HCl and NaOH were used to adjust the pH. Distilled water was used in all experiments.
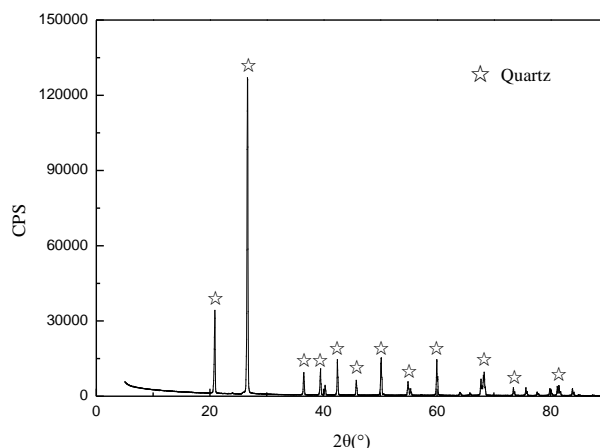
Fig. 2. X-ray diffraction spectrum of quartz

Table 1. Chemical element analysis of minerals

Element / Minerals	TFe (%)	FeO (%)	SiO_2 (%)	Al_2O_3 (%)	MgO (%)	CaO (%)	P (%)	S (%)
Hematite	67.45	≤0.15	1.25	0.29	0.03	<0.05	0.03	0.08
Quartz	0.04	– –	99.77	0.12	<0.02	<0.02	<0.01	0.007

2.3. Methods

2.3.1 Microflotation

Microflotation experiments were carried out in a 30 mL flotation cell at 1500 rpm impeller speed. The total solid content was kept 7.4% for all flotation experiments. A 2.0 g of sample composed of hematite and quartz with different particle size fractions in different proportions by weight according to test design was mixed with 25 mL of distilled water in flotation cell for 1 min. HCl or NaOH was added to maintain the pH according to test design, and the pulp was conditioned for 2 min. Different reagents were then separately added, and the pulp was conditioned for 2 min with each reagent. Distilled water was added to the test periodically to maintain the pulp level. The flotation time was fixed for 3 min at room temperature (25 °C). The froth and sink products were collected, filtered, dried, weighed, and analyzed. The same conditions (cell size, impeller type, size and speed, air flow, reagent dosage etc.) except the variables mentioned in this paper were applied to all batch tests. The tests under the same conditions were conducted in duplicate. And the results in Figures were the average value of two data.

2.3.2 Entrainment tests

The entrainment tests using quartz or hematite with different particle size fractions were performed separately in a 30 mL flotation cell at 1500 rpm impeller speed. For each test, firstly, the weight (W_0) of unused distilled water and empty tray (W_{c0}) should be recorded. And then the sample prepared was mixed with 25 g of distilled water in flotation cell for 1 min. NaOH (maintain the pH at about 11.5), calcium chloride, starch and sodium oleate were then separately added, and the pulp was conditioned for 2 min with each reagent. Open the air valve, and set the air flow rate to 4 L/min. The froth depth was controlled at about 10 mm, and the flotation froth was scraped out every 10 s. The flotation time was fixed for 0.5 to 4 min (0.5, 1, 2, 3, 4 min) at room temperature (25 °C). Distilled water was added to the test periodically to maintain the pulp level. The froth product was collected, and the tray with froth product (W_{c1}) and distilled water left (W_1) were weighed, separately. The tray with froth product were dried, weighed and recorded as (W_{c2}). The tests under the same conditions were conducted in duplicate.

The recovery of water and quartz or hematite can be calculated by Eqs. (1) and (2), respectively. The degree of entrainment of quartz or hematite can be calculated by Eq. (3).

$$R_w = \frac{W_{c1} - W_{c2}}{W_0 - W_1} \times 100\%$$ (1)

where R_w is the water recovery in froth product, %; W_0 is the weight of unused distilled watert, g; W_1 is the weight of distilled water left, g; W_{c1} is the wet weight of tray with froth product, g; W_{c2} is the dry weight of tray with froth product, g.

$$R_s = \frac{W_{c2} - W_{c0}}{2} \times 100\%$$ (2)

where R_S is the recovery of quartz or hematite in froth product, %; W_{c0} is the weight of empty tray, g; W_{c2} is the dry weight of tray with froth product, g.

$$e_g = \frac{R_s}{R_w} \times 100\%$$ (3)

where e_g is the degree of entrainment of quartz or hematite.

2.3.3 X-ray photoelectron spectroscopy

The XPS spectra of hematite or quartz with different particle size were collected from a surface of size about 2 mm × 2 mm on a spectrometer with the type of America Thermo VG ESCALAB250, where Al Kα X-rays (1486.6 eV) was adopted as sputtering source at a power of 150W (15 kV×10 mA). The chamber pressure in the analysis was 5.0×10-10 mbar during spectral acquisition. The standard C (1s) binding energy was 284.6 eV.

2.3.4 Reagent adsorption measurements

Ultraviolet spectrophotometry was performed to measure the amount of sodium oleate adsorption on the surface of hematite with different particle size fractions. Prior to the measurement of reagent adsorption amount, the standard solution of sodium oleate was scanned in the wavelength range of 190-600 nm, and the characteristic adsorption peak of sodium oleate was obtained at the wavelength of 204 nm. Then the absorbances of sodium oleate at a series of given concentrations (10 mg/L, 20 mg/L, 40 mg/L, 80 mg/L, 100 mg/L, 120 mg/L, 160 mg/L) were determined to obtain the calibration curve. After that, a 2.0 g sample of hematite with different particle size fractions was mixed with 25 ml of distilled water in a 50 ml volumetric flask for 1 min. Afterwards, sodium oleate was added and the pulp was conditioned for 5 min. The solids were filtered after standing for 3 min, and the supernatant was assembled for UV spectrometry analysis. The sodium oleate absorbance was got by employing a Spectro Flex 6600 spectrophotometer at the wave length of 204 nm. The residual concentration of sodium oleate was calculated according to the absorbance and calibration curve. On the basis of the residual concentration of sodium oleate remaining in the solution, the adsorption amount of sodium oleate on the mineral surface can be calculated by Eq. (4).

$$\Gamma = \frac{(C_0 - C) \times V}{w}$$ (4)

where Γ is the adsorption amount, mg/g; C_0 is the initial concentration of sodium oleate in the solution, mg/L; C is the residual concentration of sodium oleate in the supernatant, g/L; V is the solution volume, L; and w is the mineral weight, g.

3. Results and discussion

3.1. Microflotation experiments

3.1.1 Effect of pH value and particle size on flotation performance

Figs. 3 and 4 show the recovery of hematite and quartz with different particle size fractions as a function of pH value using sodium oleate as collector. As presented in Fig.3, relatively high recovery of hematite was observed in the pH range of 3 to 10, and the recovery reached maximum at pH about 8; the flotation response of the -106+45 μm fraction was similar to that of the -45+18 μm fraction. Nevertheless, flotation

of hematite in the -18 µm fraction was generally considered to be weak in the whole pH range, its recovery was below 20%. As shown in Fig.4, quartz mainly got collected in the sink product in the whole pH range. Quartz was hydrophilic, and could not be collected using fatty acid as collector (Araújo et al., 2005). However, the recovery of +45 µm fraction and -45µm fraction (-45+18 µm and -18 µm) reached 2% and 5%, separately.
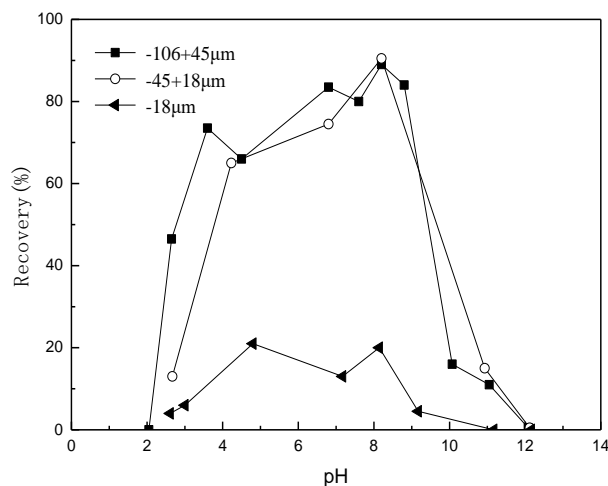
Fig. 3. Hematite recovery with different particle size fractions as a function of pH value (sodium oleate concentration: 120 mg/L)
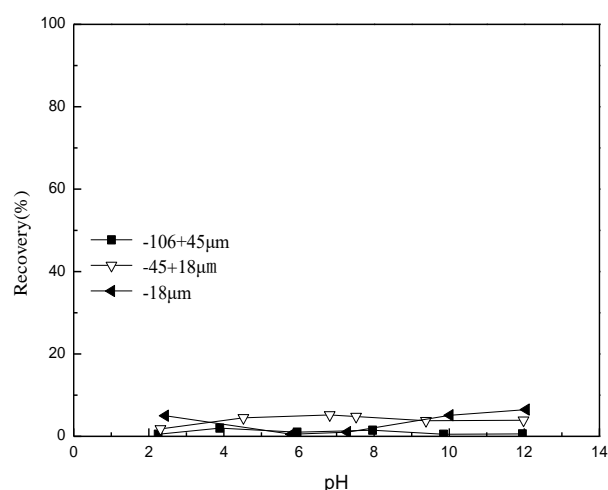
Fig. 4. Quartz recovery with different particle size fractions as a function of pH value (sodium oleate concentration: 160 mg/L)

3.1.2 Effect of regulator and particle size on flotation performance

Fatty acids and their salts, calcium ion, and starch are often employed as collector, activator of quartz, and depressant of iron minerals under strong alkaline condition, respectively (Araújo et al., 2005). Fig.5 presents the effect of starch and calcium chloride on flotation of hematite and quartz with different particle size fractions using sodium oleate as collector at pH about 11.5. Hematite with different particle size fractions mostly got collected in the sink product, but a small amount of -18 µm fraction was also found in the froth product. Meanwhile, the quartz almost got collected in the froth product. The quartz recovery in froth product greatly decreased with decreasing the particle size. The recovery of the -106+45 µm fraction reached 89%, while that of the -45+18 µm and -18 µm fractions reduced to 33% and 17.5%, separately. It is showed by the data (The Soviet academy of sciences, 1959) that the depression or activation for minerals was concerned with the particle size; the contact angle needed of particles

attached on the bubble decreased with the decrease of particle size. The smaller the particle size, the greater the reagent dosage needed (depressant or activator).
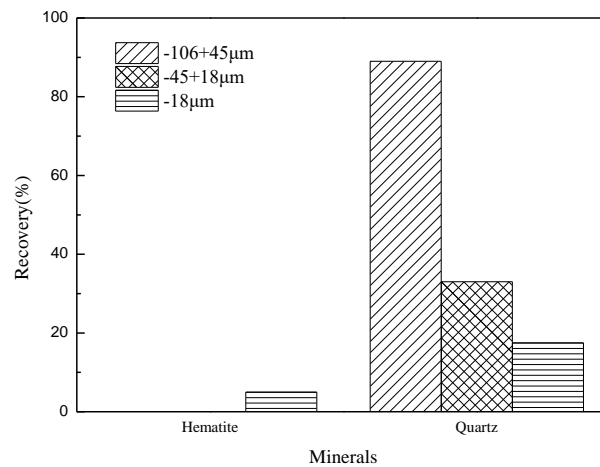
Fig. 5. Effect of starch and CaCl$_2$ on flotation of hematite and quartz with different particle size fractions (sodium oleate concentration: 160 mg/L; corn starch concentration: 60 mg/L; calcium chloride concentration: 100 mg/L; pH: 11.5)

3.1.3 Effect of particle size on separation of hematite from quartz

Fig. 6 presents the Fe grade and hematite recovery in froth product as a function of percentage of quartz with different particle size fractions using sodium oleate as collector at pH 9.0. In this figure, solid symbols indicate the Fe grade, and the hollow symbols indicate the hematite recovery. Significant change was not observed in hematite recovery in the absence and presence of quartz with different particle size fractions. Adding quartz with -45 μm fraction (-45+18 μm and -18 μm) negatively affected the Fe grade in froth product to a small extent. The curves showed a negative slope. The Fe grade in froth product decreased from 67.45% to 58.22% and 57.55%, a reduction of 9.23 and 9.90 points, when the percentage of the -45+18 μm and -18 μm fractions increased from 0% to 40%, respectively. It is consistent with the observation from Fig.5 that few quartz fines (-45 μm fraction) reported to the froth product.
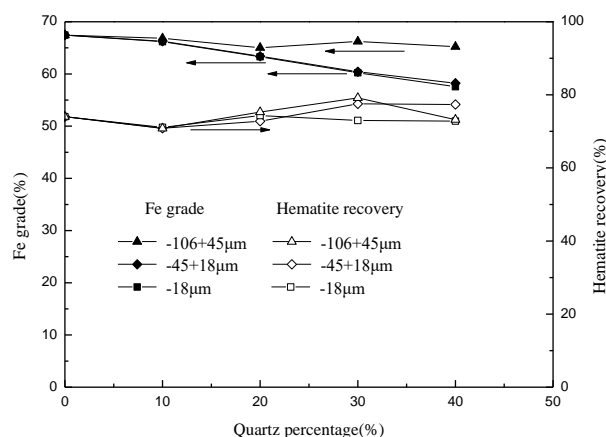
Fig. 6. Effect of quartz with different particle size fractions on hematite direct flotation (sodium oleate concentration: 120 mg/L; pH: 9.0; 2.0 g of sample: composed of hematite and quartz in different proportions by weight; particle size of hematite: -106+45 μm)

Fig. 7 shows the Fe grade and hematite recovery in sink product as a function of percentage of quartz with different particle size fractions using sodium oleate as collector, calcium chloride as activator and starch as depressant at pH 11.5. In this figure, solid symbols indicate the Fe grade, and the hollow

symbols indicate the hematite recovery. Quartz with different particle size fractions had little effect on hematite recovery in sink product, but had negative effect on Fe grade to some extent. Fe grade in sink product decreased with increasing the quartz percentage of the -45 µm fraction (-45+18 µm and -18 µm). The Fe grade in froth product decreased from 67.45% to 45.2% and 48.7%, a reduction of 22.25 and 18.75 points, when the percentage of the -45+18 µm and -18 µm fractions increased from 0% to 40%, respectively. It is consistent with the observation from Fig.5 that part of quartz fines (-45 µm fraction) reported to the sink product in the presence of sodium oleate, starch and calcium chloride.
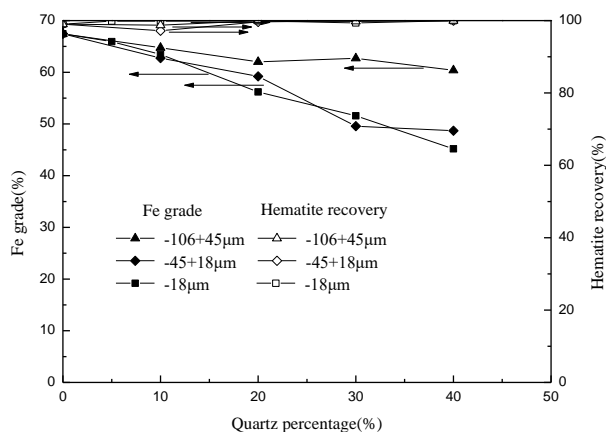
Fig. 7. Effect of quartz with different particle size fractions on hematite reverse flotation (sodium oleate concentration: 160 mg/L; corn starch concentration: 60 mg/L; calcium chloride concentration: 100 mg/L; pH: 11.5; 2.0 g of sample: composed of hematite and quartz in different proportions by weight; particle size of hematite: -106+45 µm)

Fig. 8 presents the Fe grade and hematite recovery in sink product as a function of hematite particle size in the separation of hematite from quartz in the presence of sodium oleate, calcium chloride and starch at 11.5. Hematite particle size slightly affected Fe grade in sink product, but affected hematite recovery. It is consistent with the observation from Fig.6 that part of hematite fines (-45µm fraction) reported to the froth product. It is also consistent with the observations reported by Shibata and Fuerstenau (2003) and Ng et al. (2015). This finding indicates that the presence of hematite fines has negative impact on hematite recovery.
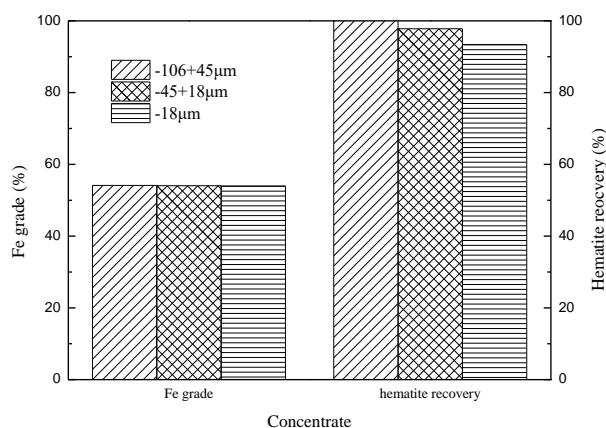
Fig. 8. Effect of hematite particle size on hematite reverse flotation (sodium oleate concentration: 160 mg/L; corn starch concentration: 60 mg/L; calcium chloride concentration: 100 mg/L; pH: 11.5; 2.0 g of sample: composed of hematite and quartz; the proportion by weight of hematite and quartz: 4:5; particle size of quartz: -106+45 µm)

3.1.4 Effect of entrainment on flotation performance

Entrainment of particles into the froth product is an important factor in the performance of the flotation process, especially for fine particle recovery. Entrainment is the unselective entrapment of fine particles

into the froth layer with the rising water (Smith and Warren, 1989) and it can be experienced by both hydrophobic and hydrophilic particles (Wang et al., 2015). It has been found that the entrained gangue recovery in a direct flotation operation is often proportional to the water recovery (Trahar, 1981).

The recovery of quartz with different particle size fractions versus water recovery at pH 9.0 in the presence of only sodium oleate is given in Fig.9 using a number of tests. The degree of entrainment of quartz with different particle size fractions at flotation time 3 min is shown in Table 2. The tests under the same conditions were conducted in duplicate. As can be seen from Fig.9, it showed a linear relationship between quartz recovery and water recovery at all size fractions; the water recovery in froth product of quartz with -18 μm, -45+18 μm and -106+45 μm increased from 1.05%, 0.89%, 0.55% to 8.67%, 7.88% and 7.26%, respectively, as the flotation time increased from 0.5 min to 4 min. These variations in water recovery explain why quartz recoveries significantly increased in these tests. The upwardly curving relationships in Fig.9 were an indication that the quartz recovery increased with the increment in water recovery; the slope of the lines (quartz with -18 μm and -45+18 μm fractions) is far greater than the slope of the line (quartz with -106+45 μm fraction), i.e. the recovery of fine particle of quartz was much higher than coarse particle when the water recovery was a certain value. The fine particles of quartz were much easier to collect into froth product with the recovery of water. The results in Table 2 indicated the degree of entrainment of fine particle was higher than that of coarse particle; the degree of entrainment of quartz with -106+45 μm fraction was only 0.12, while that of quartz with -45+18μm and -18 μm fractions reached 0.58 and 0.96, separately. This agrees with studies presented by Neethling and Cilliers (2009), Kirjavainen (1996), Melo and Laskowski (2007) and Lima et al. (2016). Therefore, this magnitude of change in the degree of entrainment could result in a significant change in the concentrate grade in hematite direct flotation as demonstrated by simulations performed by Wang et al. (2016), which was in line with results from Fig. 6.
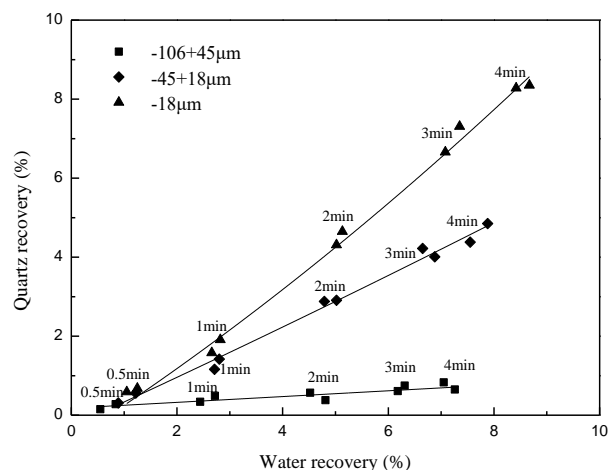
Fig. 9. The recovery of quartz with different particle size fractions versus water recovery (pH=9.0; sodium oleate concentration: 120 mg/L; flotation time: 0.5, 1, 2, 3, 4 min)

Table 2 Degree of entrainment of quartz with different particle size fractions

Particle size of quartz(μm)	Degree of entrainment
-106+45	0.12
-45+18	0.58
-18	0.96

Fig. 10 shows the hematite recovery in froth product versus water recovery in the presence of sodium oleate, calcium chloride and starch at 11.5. The data under the same conditions were also in duplicate. The degree of entrainment of hematite with different particle size fractions at flotation time 3 min is shown in Table 3. It also showed a strong correlation between hematite recovery with different particle size fractions and water recovery which varied significantly in the experiments. With the increase of flotation time, both the recovery of water and -18 μm fractions strongly increased, but that of +18 μm

fraction slightly increased. Hematite with -18 μm fraction had highest degree of entrainment, which was easy to report to the froth product, thereby negatively affecting the hematite recovery in sink product. These results are consistent with the results from Figs. 5 and 8, and observations reported by Lima et al. (2016).
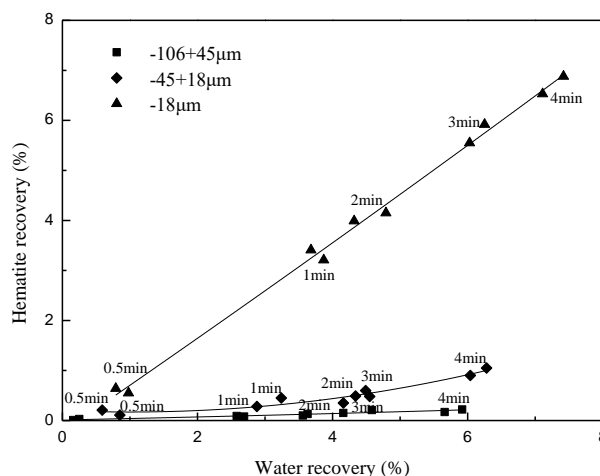
Fig. 10. The recovery of hematite with different particle size fractions versus water recovery (pH: 11.5; sodium oleate concentration: 160 mg/L; corn starch concentration: 60 mg/L; calcium chloride concentration: 100 mg/L; flotation time: 0.5, 1, 2, 3, 4 min)

Table 3. Degree of entrainment of hematite with different particle size fractions

Particle size of hematite(μm)	Degree of entrainment
-106+45	0.04
-45+18	0.15
-18	0.93

3.2. X-ray photoelectron spectroscopy (XPS) analysis

Table 4 shows the results of XPS analysis of hematite surface with different particle size fractions at pH 11.5. For hematite, Fe element relative concentration increased with decreasing the particle size, indicating that fine hematite particles had larger surface area and more bonding sites for sodium oleate adsorption, thereby consuming more sodium oleate.

Table 4. XPS analysis of mineral surface with different particle size fractions

Minerals	Particle size (μm)	Surface Elements	Electron binding energy (eV)	Element relative concentration (%)
	-106+45	C1s	284.60	52.36
		O1s	529.64	40.09
		Fe2p	710.34	7.56
	-45+18	C1s	284.60	44.19
Hematite		O1s	529.59	46.83
		Fe2p	710.88	8.98
	-18	C1s	284.60	35.01
		O1s	530.03	53.25
		Fe2p	710.75	11.73

3.3. Reagent adsorption measurements

Table 5 gives the adsorption capacity of sodium oleate on hematite and quartz in direct flotation and in reverse flotation, respectively. In direct flotation, sodium oleate (120 mg/L) was used as collector at pH

about 9.0. In reverse flotation, sodium oleate (160 mg/L) was used as collector, calcium chloride (100 mg/L) was used as activator of quartz, and corn starch (60 mg/L) was used as depressant of hematite at pH about 11.5. The results from Table 5 and Fig.9 indicated that quartz was hydrophilic and could not be collected using sodium oleate as collector, the entrainment of quartz could result in a reduction in the concentrate grade in hematite direct flotation. The results from Table 5 and Fig.10 showed that hematite was hydrophilic and could not be collected using sodium oleate as collector in the presence of corn starch, the entrainment of fine hematite could negatively affect the hematite recovery in sink product in hematite reverse flotation.

Fig.11 shows the sodium oleate adsorption capacity on hematite with different particle size as a function of sodium oleate concentration at pH about 9.0. It showed a linear relationship between sodium oleate adsorption capacity and sodium oleate concentration; the finer hematite particle size, the more sodium oleate adsorption capacity, which was consistent with the XPS analysis results that finer hematite had more bonding site for sodium oleate adsorption. To further find the reason of difficulty in floating fine particles, then the collision and attachment probability calculation and flocculation flotation were carried out.

Table 5. Adsorption capacity of sodium oleate on hematite and quartz

Flotation	Adsorption capacity of sodium oleate (mg/g)	
	Hematite	Quartz
Direct flotation	0.49	0.001
Reverse flotation	0.02	1.89

3.4. Collision and attachment probability calculation

The interaction between particles and air bubbles is a key element to effectively recover valuable minerals via the flotation process (Phan et al., 2003). The study of collision and attachment between solid particle and air bubbles in aqueous solutions is the key to understanding froth flotation.
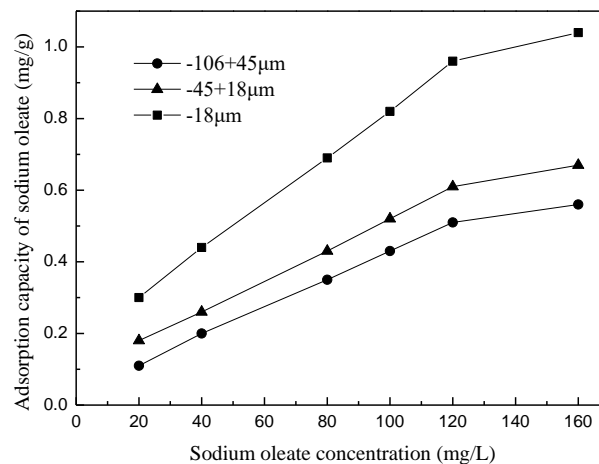
Fig. 11. Sodium oleate adsorption capacity on hematite with different particle size

The probability (Pc) of bubble-particle collision in the pulp phase of a flotation cell can be given by:

$$P_c = B_c \left(\frac{d_p}{d_b} \right)^n \tag{5}$$

where P_c is the probability of bubble-particle collision; d_p is the diameter of the particle; d_b is the diameter of the bubble and B_c and n are the parameters that vary with Reynolds numbers. Table 6 gives

these values for the three different flow regimes considered, i.e., Stokes, intermediate and potential flows (Yoon, 2000; Gaudin, 1957; Yoon and Luttrell, 1989; Weber and Paddock, 1983; Sutherland, 1948).

Table 6. Value of Bc and n for different flow conditions (Yoon, 2000)

Flow conditions	Bc	n
Stokes (Gaudin, 1957)	$3/2$	2
Intermediate (Yoon) (Yoon and Luttrell, 1989)	$\dfrac{3}{2}+\dfrac{4Re_b^{0.72}}{15}$	2
Intermediate (weber) (Weber and Paddock, 1983)	$\dfrac{3}{2}\left(1+\dfrac{\dfrac{3}{16}Re_b}{1+0.249\,Re_b^{0.56}}\right)$	2
Potential (Sutherland, 1948)	3	1
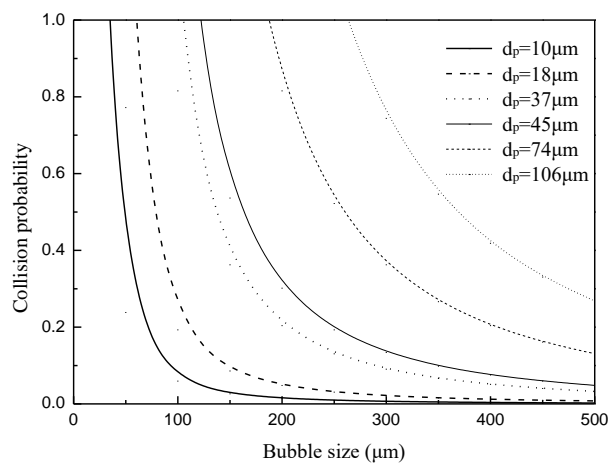
Fig. 12. Collision probability as a function of bubble size and particle size
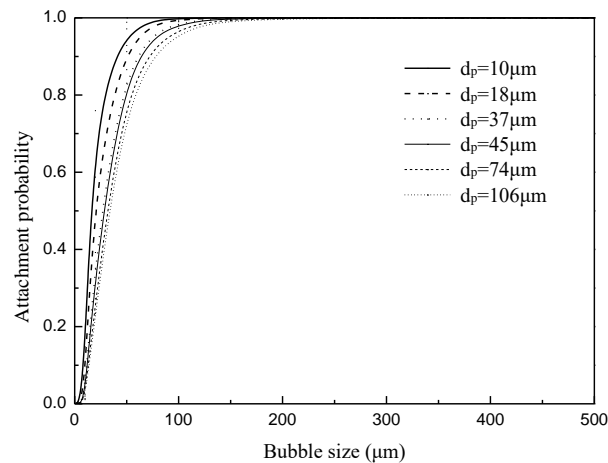
Fig. 13. Attachment probability as a function of bubble size and particle size

The probability of collision was calculated for different particle sizes (10, 18, 37, 45, 74, 106 µm) and bubble size according to the formula (5) and intermediate (Yoon) equation. As shown in Fig.12, the collision probability of particles decreased with increasing the bubble size; the coarse particles had higher collision probability than fine particles at constant bubble size. These results indicated that difficulty in floating fine particles was mostly due to low collision probability.

For predicting attachment, probability under turbulent conditions, can use below equation (Yoon, 2000):

$$P_a = \sin^2 \left[2 \arctan \exp \frac{-\left(45 + 8\,\mathrm{Re}_b^{0.72}\right) v_b t_i}{15 d_b \left(d_b / d_p + 1\right)} \right] \qquad (6)$$

where P_a is the probability of attachment; d_p is the diameter of particle; d_b is the diameter of bubble; t_i is induction time (30s); v_b is the bubble rise velocity (0.09 m/s) (Yang, 2017).

As shown in Fig.13, the attachment probability of particles increased with increasing the bubble size; the fine particles had higher attachment probability than coarse particles at constant bubble size. These results indicated that high entrainment degree for fine particle was mostly due to high attachment probability.

3.5. Flocculation flotation of fine hematite and quartz

Microflotation experiments of fine hematite (-18 μm fraction) were carried out using sodium oleate as collector (120mg/L) at pH 9 at 1500 rpm and 2500 rpm impeller speed, respectively. Their particle size distribution and hematite recovery were shown in Fig. 14 and Table 7 separately. The result from Fig.14 showed that the particle size of hematite increased with improving impeller speed from 1500 rpm to 2500 rpm. Meanwhile, the recovery of fine hematite increased from 10.53% to 48.05%. The result of adsorption capacity of hematite (-18 μm fraction) from Fig.11 and the results from Figs. 12 and 14, and Table 6 indicated that difficulty in floating fine particles was mostly due to low collision probability. Therefore, the collision probability could be improved through increasing the particle size.

Microflotation experiments of fine quartz (-37 μm fraction) were carried out in the presence of sodium oleate (160 mg/L), calcium chloride (100 mg/L) and corn starch (60 mg/L) at pH 11.5 at 1500 rpm and 2500 rpm impeller speed, separately. The particle size distribution and quartz recovery were shown in Fig. 15 and Table 8, respectively. The result from Fig.15 showed that the particle size of quartz increased when the impeller speed increased from 1500 rpm to 2500 rpm. Meanwhile, the recovery of fine quartz increased from 28.44% to 52.21%. The result indicated the reason that the quartz recovery in froth product greatly decreased with decreasing the particle size in the presence of sodium oleate, calcium chloride and starch was mostly due to low collision probability of fine quartz.
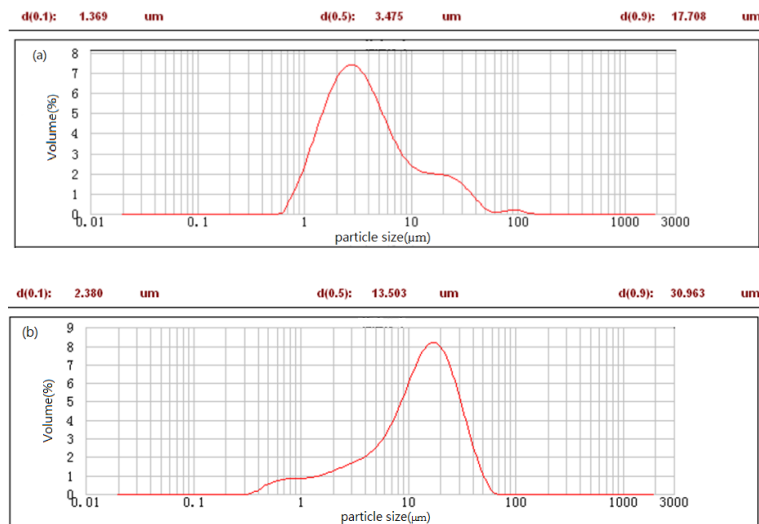
Fig. 14. Particle size distribution of fine hematite at 1500 rpm (a) and 2500 rpm (b) impeller speed (particle size of hematite: -18 μm; pH: 9; sodium oleate concentration: 120 mg/L)

Table 7. Hematite recovery at 1500 rpm and 2500 rpm impeller speed

pH	Sodium oleate (mg/L)	Impeller speed (rpm)	Hematite recovery (%)
8.92	160	1500	10.53
9.01	160	2500	58.05

Table 8. Quartz recovery at 1500 rpm and 2500 rpm impeller speed

pH	Sodium oleate (mg/L)	Calcium chloride (mg/L)	Corn starch (mg/L)	Impeller speed (rpm)	Quartz recovery (%)
8.92	160	100	60	1500	28.44
9.01	160	100	60	2500	52.21
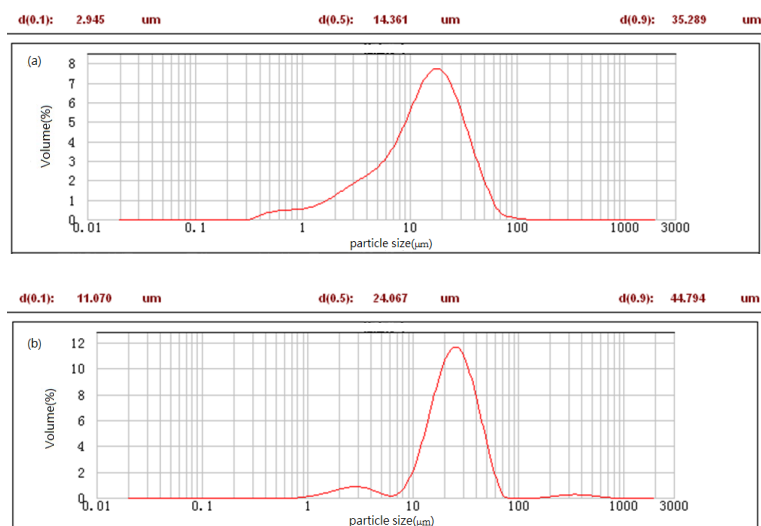
Fig. 15. Particle size distribution of fine quartz at 1500 rpm (a) and 2500 rpm (b) impeller speed (particle size of quartz: -37 μm; pH: 11.5; sodium oleate concentration: 160 mg/L; calcium chloride: 100 mg/L; corn starch: 60 mg/L)

4. Conclusions

(1) The floatability of minerals with different particle size fractions is different. The flotation of hematite with -18 μm fraction is weaker than +18 μm fraction in the presence of only sodium oleate as a result of more bonding site, more sodium oleate adsorption and lower collision probability; on the contrary, the recovery of -18 μm fraction is higher than that of +18 μm fraction in the presence of sodium oleate, calcium chloride and starch because of fine hematite entrainment.

(2) The quartz recovery in froth product in the presence of only sodium oleate results from entrainment. The entrainment degree of fine particle is higher than that of coarse particle. With decreasing the particle size, the quartz recovery in froth product greatly decreased in the presence of sodium oleate, calcium chloride and starch, due to lower collision probability.

(3) No matter in the direct flotation (only sodium oleate) or in the reverse flotation (sodium oleate, calcium chloride and sodium oleate), the quartz with different particle size has little impact on hematite recovery but -45 μm fraction negatively affected Fe grade of concentrate; in direct flotation, the Fe grade in froth product dropped off due to the fine quartz entrainment; while in reverse flotation, the Fe grade in sink product dropped off as a result of difficulty in floating fine (-45 μm fraction) quartz particles, which is due to lower collision probability. The presence of hematite fines also negatively affects the hematite recovery due to fine hematite particle entrainment.

Acknowledgements

References

ARAÚJO, A.C., VIANA, R.P.M., PERES, A.E.C., 2005. *Reagents in iron ores flotation*. Miner. Eng. 18, 219-224.

CHEN, W., ZHANG, L.G., 2013. *Technological progress in processing low-grade complicated refractory iron ores.* Nonferrous Met. (Miner. Process. Sect.). (c1), 19-23.

FORBES, E., 2011. *Shear selective and temperature responsive flocculation: a comparison of fine particle flotation.* Int. J. Miner. Process. 99(1/2/3/4), 1-10.

GAUDIN, A.M., 1957. *Flotation.* 2nd ed., Mc Graw-Hill, New York.

HAN, Y.X., SUN, Y.S., YI, Y.J., GAO, P., 2015. *New development on mineral processing technology of iron ore resources in China.* Metal mine. 44(2), 1-11.

KAR, B., SAHOO, H., RATH, S., DAS, B., 2013. *Investigations on different starches as depressants for iron ore flotation.* Miner. Eng. 49, 1-6.

KIRJAVAINEN, V.M., 1996. *Review and analysis of factors controlling the mechanical flotation of gangue minerals.* Int. J. Miner. Process. 46, 21-34.

LEISTNER, T., PEUKER, U.A., RUDOLPH, M., 2017. *How gangue particle size can affect the recovery of ultrafine and fine particles during froth flotation.* Miner. Eng. 109, 1-9.

LI, H.Q., FENG, Q.M., YANG, S.Y., OU, L.M., LU, Y., 2014. *The entrainment behaviour of sericite in microcrystalline graphite flotation.* Int. J. Miner. Process. 127, 1-9.

LI, L.X., HAO, H.Q., YUAN Z.T., LIU, J.T.,2017. *Molecular dynamics simulation of siderite-hematite-quartz flotation with sodium oleate.* Applied Surface Science, 2017, (419): 557-563

LIMA, N.P., SOUZA PINTO, T.C., TAVRES, A.C., SWEET, J., 2016. The entrainment effect on the performance of iron ore reverse flotation. Miner. Eng. 96-97, 53-58.

LIU, W.G., LIU, W.B, DAI, S.J., WANG, B.Y., 2018. Adsorption of bis(2-hydroxy-3- chloropropyl) dodecylamine on quartz surface and its implication on flotation. Results in Physics, 2018, 9C, 1096-1101.

LUO, X.M., YIN, W.Z., SUN, C.Y., WANG, N.L., MA, Y.Q., WANG, Y.F., 2016. Improved flotation performance of hematite fines by using citric acid as a novel dispersant. Int. J. Min. Met. Mater. 23, 1119-1125.

MA, X., MARQUES, M., GONTIJO, C., 2011. *Comparative studies of reverse cationic/anionic flotation of Vale iron ore.* Int. J. Miner. Process. 100 (3/4), 179-183.

MELO, F., LASKOWSKI, J.S., 2007. *Effect of frothers and solid particles on the rate of water transfer to froth.* Int. J. Miner. Process. 84, 33-40.

NEETHLING, S.J., CILLIERS, J.J., 2009. *The entrainment factor in froth flotation: model for particle size and other operating parameter effects.* Int. J. Miner. Process. 93, 141-148.

NG, W.S., SONSIE, R., FORBES, E., FRANKS, G.V., 2015. *Flocculation flotation of hematite fines with anionic temperature responsive polymer acting as a selective flocculant and collector.* Miner. Eng. 77(1), 64-71.

NORORI-MCCORMAC, A., BRITO-PARADA, P.R., HADLER, K., COLE, K., CILLIERS, J.J., 2017. *The effect of particle size distribution on froth stability in flotation.* Sep. Purif. Technol. 184, 240-247.

PÉREZ-GARIBAY, R., RAMÍREZ-AGUILERA, N., BOUCHARD, J., RUBIO, J., 2014. *Froth flotation of sphalerite: Collector concentration, gas dispersion and particle size effects.* Miner. Eng. 57, 72-78.

PHAN, C.M, NGUYEN, A.V, MILLER, J.D., EVANS, G.M., JAMESON, G.J., 2003. *Investigations of bubble-particle interactions.* Int. J. Miner. Process. 72(1-4), 239-254.

PITA, F., CASTILHO, A. 2017. *Separation of plastics by froth flotation. The role of size, shape and density of the particles.* Waste Manage. 60, 91-99.

QIU, G.Z., HU, Y.H., WANG, D.Z., 1994. *The mechanism of ultrafine hematite carrier flotation.* Nonferrous Met. 46(4), 23-28.

SMITH, P.G., WARREN, L.J., 1989. *Entrainment of particles into flotation froths.* Miner. Process. Extr. Metall. Rev. 5, 123-145.

SHIBATA, J., FUERSTENAU, D.W., 2003. *Flocculation and flotation characteristics of fine hematite with sodium oleate.* Int. J. Miner. Process. 72, 25-32.

SHRIMALI, K., ATLURI, V., WANG, Y., BACCHUWAR, S., WANG, X., MILLER, J.D., 2018. *The nature of hematite depression with cornstarch in the reverse flotation of iron ore.* J. Colloid Interface Sci., 524, 337-349.

SHRIMALI, K., JIN, J., HASSAS, B.V., WANG, X., MILLER, J.D., 2016a. *The surface state of hematite and its wetting characteristics.* J. Colloid Interface Sci., 477, 16-24.

SHRIMALI, K., MILLER, J.D., 2016b. *Polysaccharide depressants for the reverse flotation of iron ore.* Trans. Indian Inst. Met., 69(1), 83-95.

SUTHERLAND, K.L., 1948. *Physical chemistry of flotation. XI. Kinetics of the flotation process.* J. Phys. Chem. 52, 394-425.

TRAHAR, W.J., 1981. *A rational interpretation of the role of particle size in flotation*. Int. J. Miner. Process. 8, 289-327.

THE SOVIET ACADEMY of SCIENCES, 1959. *Non-metallic mineral flotation process*. Construction engineering press.

VIEIRA, A.M., PERES, A.E.C., 2007. *The effect of amine type, pH, and size range in the flotation of quartz*. Miner. Eng. 20, 1008-1013.

WANG, L., PENG, Y., RUNGE, K., 2016. E*ntrainment in froth flotation: the degree of entrainment and its contributing factors*. Powder Technol. 288, 202-211.

WANG, L., PENG, Y., RUNGE, K., BRADSHAW, D.J., 2015. *A review of entrainment: mechanisms, contributing factors and modelling in flotation*. Miner. Eng. 70, 77-91.

WEBER, M.E., PADDOCK, D., 1983. *Interceptional and gravitational collision efficiencies for single collectors at intermediate Reynolds numbers*. J. Colloid Interface Sci. 94, 328-335.

YANG, H.F., TANG, Q.Y., WANG, C.L., ZHANG, J.L., 2013. *Flocculation and flotation response of Rhodococcus erythropolis to pure minerals in hematite ores*. Miner. Eng. 45, 67-72.

YANG, B., 2017. *Research on entrainment behavior of chlorite in the flotation process of hematite* (MSC thesis). Northeast University, China.

YIN, W.Z., MA, Y.Q., WANG, N.L., LUO, X.M., 2013. Research on dispersion flotation of iron ores based on mineral interactive effect. Nonferrous Met. (z1). 146-150.

YIN, W.Z., WANG, J.Z., 2014. *Effects of particle size and particle interactions on scheelite flotation*. Trans. Nonferrous Met. Soc. China. 24, 3682-3687.

YIN, W.Z., YANG, X.S., ZHOU, D.P., LI, Y.J., LV, Z.F., 2011. *Shear hydrophobic flocculation and flotation of ultrafine Anshan hematite using sodium oleate*. Trans. Nonferrous Met. Soc. China. 21(3), 652-664.

YOON, R.H., 2000. *The role of hydrodynamic and surface forces in bubble-particle interaction*. Int. J. Miner. Process. 58 (1-4), 129-143.

YOON, R.H., LUTTRELL, G.H., 1989. *The effect of bubble size on fine particle flotation*. Miner. Process. 5, 101-122.